THE JOURNAL OF BIOLOGICAL CHEMISTRY
Vol. 278, No. 2, Issue of January 10, pp. 791–799, 2003
Printed in U.S.A.

Biochemical and Genetic Evidence for the Involvement of Yeast Ypt6-GTPase in Protein Retrieval to Different Golgi Compartments*

Received for publication, September 6, 2002, and in revised form, October 18, 2002
Published, JBC Papers in Press, October 24, 2002, DOI 10.1074/jbc.M209120200

Zongli Luo and Dieter Gallwitz‡

From the Max Planck Institute for Biophysical Chemistry, Department of Molecular Genetics, D-37070 Göttingen, Germany

Yeast Ypt6p, the homologue of the mammalian Rab6 GTPase, is not essential for cell viability. Based on previous studies with *ypt6* deletion mutants, a regulatory role of the GTPase either in protein retrieval to the *trans*-Golgi network or in forward transport between the endoplasmic reticulum (ER) and early Golgi compartments was proposed. To assess better the primary role(s) of Ypt6p, temperature-sensitive *ypt6* mutants were generated and analyzed biochemically and genetically. Defects in *N*-glycosylation of proteins passing the Golgi and of Golgi-resident glycosyltransferases as well as protein sorting defects in the *trans*-Golgi were recorded shortly after functional loss of Ypt6p. ER-to-Golgi transport and protein secretion were delayed but not interrupted. Mis-sorting of the vesicular SNARE Sec22p to the late Golgi was also observed. Combination of the *ypt6-2* mutant allele with a number of mutants in forward and retrograde transport between ER, Golgi, and endosomes led to synthetic negative growth defects. The results obtained indicate that Ypt6p acts in endosome-to-Golgi, in *intra*-Golgi retrograde transport, and possibly also in Golgi-to-ER trafficking.

Intercompartmental transport of proteins in secretion and endocytosis is affected by a variety of vesicle populations, each having its own biochemical identity. Generation of transport vesicles at different donor compartments and their fusion with defined target membranes follow general principles and require protein machines made up of related and evolutionarily conserved proteins that are, however, specific for each transport step (1, 2). Among the proteins that confer specificity and directionality to vesicular trafficking are Ras-like GTPases of the Ypt/Rab family (3–6). In the yeast *Saccharomyces cerevisiae*, this GTPase family has 11 members of which only those that act in forward transport through the secretory pathway (Ypt1p, Sec4p, and the pair of apparently redundant Ypt31/Ypt32-GTPases) are essential for cell viability (3). Of the nonessential ones, Ypt6p, the homologue of the mammalian Rab6 GTPases, has been implicated in having a role in the retrieval of proteins from endosomes to the *trans*-Golgi network (7–10) or in anterograde (11, 12) and retrograde (9) Golgi transport.

The divergent views on Ypt6p function were based on the results of the initial studies (7, 8, 11, 12) using *ypt6* deletion or truncation mutants. Such mutants were found to be growth-inhibited at elevated temperature, to partially mis-sort proteins in the *trans*-Golgi network already at permissive temperature, and to moderately interfere with protein secretion at nonpermissive conditions (7, 11). Temperature sensitivity of *ypt6* deletion mutants allowed us to isolate multicopy suppressors of which one, *SYS1* (7), could also rescue another protein mis-sorting mutant, *ric*Δ (9), later shown to be defective in the nucleotide exchange factor for Ypt6p (13). Cells lacking Ypt6p accumulate transport vesicles (8) of which at least a fraction may be derived from endosomes and destined to fuse with late Golgi membranes (10). On the other hand, temperature-sensitive growth of *ypt6* deletion mutants can be overcome efficiently by raising the intracellular level of Ypt1p (12), the GTPase required for ER[1]-to-Golgi (14) and early Golgi transport (15). Furthermore, partial suppression of growth defects of *ypt6* and *ric1* null mutants by high expression of a variety of genes that are known to act in either forward or retrograde Golgi transport have led to the assumption that Ypt6p might participate in regulating more than one transport step (9). This would in fact mirror the situation in mammalian cells where the homologue of yeast Ypt6p, Rab6, initially thought to function only in *intra*-Golgi transport (16), is also required for recycling of proteins between endosomes and the TGN (17). The notable difference, however, is that although yeast has only one form of Ypt6p, mammalian cells are endowed with two Rab6 isoforms that apparently act sequentially in transport from endosomes to the early Golgi (17) and even to the ER (18).

As previous studies with *ypt6* deletion mutants have the inherent problem that adaptive changes in the physiology of such cells might obscure the true lesions caused by functional loss of the GTPase, we sought to investigate Ypt6p function with the help of conditional mutants. The data obtained from genetic interactions and from experiments following the kinetics of protein transport and sorting as well as the state of protein glycosylation at permissive and nonpermissive conditions are best explained by Ypt6p acting both in recycling of proteins from endosomes to the Golgi and from late to early Golgi compartments.

EXPERIMENTAL PROCEDURES

Yeast Strains, Genetic Methods, and Plasmids—Yeast strains used in this study are listed in Table I. Yeast transformations, mating, sporulation, and tetrad analyses were performed using standard techniques (19, 20). c-Myc epitope tagging of ORFs was performed as described previously (21). To produce pKS-YPT6-URA3 for site-directed mutagenesis, the 1.4-kb *Xba*I *YPT6* gene fragment from pRS315-YPT6 was

* This work was supported by the Max Planck Society and by grants from the Deutsche Forschungsgemeinschaft, the Fonds der Chemischen Industrie, and the Human Frontier Science Program (to D. G.). The costs of publication of this article were defrayed in part by the payment of page charges. This article must therefore be hereby marked "*advertisement*" in accordance with 18 U.S.C. Section 1734 solely to indicate this fact.

‡ To whom correspondence should be addressed. Tel.: 49-551-201-1496; Fax: 49-551-201-1718; E-mail: Dieter.Gallwitz@mpi-bpc.mpg.de.

[1] The abbreviations used are: ER, endoplasmic reticulum; TGN, *trans*-Golgi network; ORF, open reading frame; PNGase, peptide: *N*-glycosidase; COP, coat protein; SNARE, soluble NSF (*N*-ethylmaleimide-sensitive factor) attachment protein receptor; WT, wild type; ALP, alkaline phosphatase.

TABLE I
Strains used in this study

Strain	Genotype	Source
MSUC-1A	*MAT**a** ura3 his3 leu2 trp1 ade8*	This laboratory
MSUC-3D	*MATα ura3 his3 leu2 trp1 lys2*	This laboratory
ZLY1	MSUC-3D, *ypt6-1-URA3*	This study
ZLY2	MSUC-3D, *ypt6-2-URA3*	This study
ZLY2-K	MSUC-3D, *ypt6-2-loxP-KanMX-loxP*	This study
ZLY2-1A	MSUC-1A, *ypt6-2-URA3*	This study
ZLY3	MSUC-3D, *ypt6-3-URA3*	This study
ZLY4	MSUC-3D, *ypt6::HIS3*	This study
ZLY45	MSUC-3D, *tlg2::HIS3*	This study
ZLY361	MSUC-3D, *vps35::HIS3*	This study
ZLY351	MSUC-3D, *OCH1-6His-2Myc-loxP-KanMX-loxP*	This study
ZLY352	MSUC-3D, *MNN1-6His-2Myc-loxP-KanMX-loxP*	This study
ZLY353	MSUC-3D, *MNN9-6His-2Myc-loxP-KanMX-loxP*	This study
ZLY354	MSUC-3D, *ANP1-6His-2Myc-loxP-KanMX-loxP*	This study
ZLY355	MSUC-3D, *VAN1-6His-2Myc-loxP-KanMX-loxP*	This study
ZLY356	MSUC-3D, *ypt6-2-URA3, OCH1-6His-2MYC-loxP-KanMX-loxP*	This study
ZLY357	MSUC-3D, *ypt6-2-URA3, MNN1-6His-2MYC-loxP-KanMX-loxP*	This study
ZLY358	MSUC-3D, *ypt6-2-URA3, MNN9-6His-2MYC-loxP-KanMX-loxP*	This study
ZLY359	MSUC-3D, *ypt6-2-URA3, ANP1-6His-2MYC-loxP-KanMX-loxP*	This study
ZLY360	MSUC-3D, *ypt6-2-URA3, VAN1-6His-2MYC-loxP-KanMX-loxP*	This study
ZLY184	*MATα ura3 his4 leu2 sec23-1 OCH1-6His-2MYC-loxP-KanMX-loxP*	This study
ZLY185	*MATα ura3 his4 leu2 sec23-1 MNN1-6His-2Myc-loxP-KanMX-loxP*	This study
RPY18	MSUC-1A, *sec24-11*	Peng et al. (55)
RPY41	MSUC-3D, *sed5-1*	This laboratory
RPY108	MSUC-3D, *sly1^{ts}*	This laboratory
RPY116	MSUC, *MATa ura3 his3 leu2 trp1 lys2 sec35-1*	This laboratory
YXY12α	MSUC-3D, *yip1-2-TRP1*	Yang *et al.* (40)
YXY136	MSUC-3D, *ypt1^{A136D}-LEU2*	This laboratory
YLX15	MSUC-3D, *ypt32^{A141D}-HIS3 ypt31::KanMX*	This laboratory
BSH-1B	*MAT**a** ura3 his3 leu2 suc2-Δ9 bet1-1*	This laboratory
CTY1-1A	*MAT**a** ura3 his3 lys2 sec14-1*	S.D. Emr (UC San Diego)
GWY67	*MATα leu2-3 112 ura3-52 trp1 uso1-1*	G. Waters (Princeton University)
MB7	*MATα leu2 ura3 his4 suc2-Δ9 sec7-1*	M. Bielefeld (Universitat Düsseldorf)
YTX50	*MAT**a** ura3 leu2 his4 sec18-1*	T. Sommer (Max-Delbruck-Centrum Berlin)
PC70	*MATα ura3 leu2 trp1 ret1-1*	P. Cosson (University of Geneva)
PC130	*MAT**a** ura3 leu2 his4 lys2 ret2-1*	P. Cosson
PC159	*MAT**a** ura3 leu2 his4 trp1 suc2-Δ9 ret3-1*	P. Cosson
RH227-3A	*MAT**a** ura3 his4 leu2 sec23-1*	H. Riazman (Biocenter, Basel)
RH236-3A	*MATα ura3 his4 leu2 sec20-1*	H. Riezman
RH237-1A	*MAT**a** ura3 his4 leu2 lys2 sec12-4*	H. Riezman
RH239-5A	*MATα ura3 his4 leu2 lys2 sec21-1*	H. Riezman
S27P4-9C	*MATα leu2 ura3 lys2 pep4::HIS3 sec27-1*	This laboratory

inserted into the *Xba*I site of pBluescript II KS$^+$ (Stratagene). The *Hin*dIII *URA3* gene fragment from YEp24 (New England Biolabs) was inserted into the *Stu*I site of *YPT6* created 22 bp behind the stop codon. To create pYX242-SEC35, the coding sequence of *SEC35* gene with a newly created *Nco*I site at the 5′ end and an *Xho*I site at the 3′ end was amplified by PCR from yeast genomic DNA using *Pfu* DNA polymerase (Stratagene). This fragment was inserted into the *Nco*I-*Xho*I sites of pYX242 (R&D Systems). Plasmids pRS315-YPT6 and pRS325-SYS1 were constructed as described previously (7); pRS326-YPT1 was from R. Peng (this laboratory), and pWB-Acycα (*P$_{CYC1}$-SEC22*-myc-α factor, *CEN*, *URA3*) was from H. D. Schmitt (this laboratory).

Site-directed Mutagenesis and Gene Disruption—YPT6 mutant genes encoding the GTPase with either K125N, G139D, or A143D substitution were generated by site-directed mutagenesis using QuickChange™ mutagenesis kit (Stratagene) on the plasmid pKS-YPT6-URA3. After mutation, an *Xba*I fragment of the mutated *YPT6* gene with the adjacent *URA3* gene as selection marker was integrated into the *YPT6* locus of a haploid strain, and mutants were selected on SD-Ura plates. Chromosomal mutations were verified by sequencing the PCR products generated from genomic DNA of selected *ypt6* mutants. Disruption of genes was performed by PCR-based replacement using the *HIS3* gene amplified from plasmid pRS303 (22) to replace the respective ORFs as described (23).

Protein Extraction, PNGase F Treatment, and Immunoblotting—Yeast cells were grown at 25 °C to mid-log phase. Ten A_{600} units of cells were collected before and after incubation at 37 or 39 °C for different times, resuspended in 150 μl of SDS sample buffer containing proteinase inhibitors, and lysed by vortexing for 10 min at 4 °C with glass beads. For PNGase F digestion, cells were collected, spheroplasted, and gently lysed in HEPES buffer. The lysates were then centrifuged at 100,000 × *g* for 2 h at 4 °C; the pellets were resolved in 0.5% SDS buffer containing 1% β-mercaptoethanol, and digestions were done according to the protocols advertised by the supplier (New England Biolabs). For immunoblotting, proteins were resolved by SDS-PAGE, transferred to nitrocellulose membranes, and probed with polyclonal antibodies against c-Myc epitope (Santa Cruz Biotechnology), CPY, ALP, or chitinase.

Cell Labeling, Immunoprecipitation, and Invertase Assay—Cell labeling and immunoprecipitations were performed as described previously (24) with the following modifications. Cells were grown in synthetic minimal medium containing 2% glucose (SMM) (25) to mid-log phase and labeled with Tran^{35}S-label (ICN) in either SD medium supplemented with the required amino acids or in SMM containing 1 M sorbitol and 1 mg/ml ovalbumin. Labeling in SMM was terminated by adding 10 mM NaN_3/NaF and in SD medium by 2× spheroplast buffer (50 mM Tris, pH 7.5, 2 M sorbitol, 20 mM NaN_3/NaF, 20 mM dithiothreitol). Spheroplasts were made by adding 10 μg of zymolase 100-T (Seikagaku Kogyo) per 1 A_{600} unit of cells and incubating for 45 min at 30 °C. Secretion of proteins into the medium was assayed as described (26). Invertase activity staining was carried out as described previously (27).

Sucrose Gradient Fractionation—Yeast cells were grown at 25 °C to mid-log phase and then shifted to 37 °C for 1 h. 150 A_{600} units of cells were collected. Lysates were prepared and subjected to sucrose gradient centrifugation as described (28). Thirteen fractions were collected manually from the top of the gradient and mixed with one-fifth volume of 6× SDS sample buffer and incubated at 95 °C for 10 min prior to SDS-PAGE. Immunoblots were performed using specific antibodies against Kar2p, Emp47p, CPY, ALP, Anp1p, and the c-Myc epitope.

RESULTS

Growth Phenotype of ypt6 Temperature-sensitive Mutants—Ypt6p is not required to sustain cell growth and multiplication.

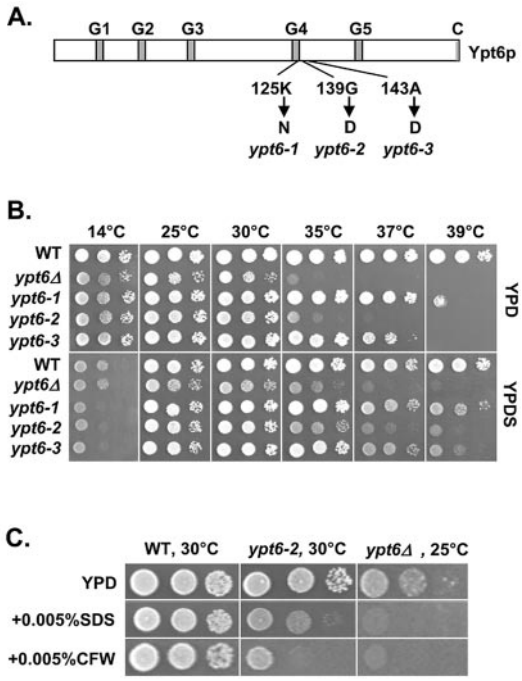

FIG. 1. **Generation and growth phenotype of *ypt6* mutants.** *A*, location of single amino acid substitutions in Ypt6p of three different mutants. *G1–5*, conserved GTPase domains; *C*, conserved C-terminal cysteine residue. *B*, 3.0 μl of 10-fold diluted log-phase cultures, starting with 3×10^6 cells/ml, were spotted onto YPD or YPDS (YPD plus 1 M sorbitol) plates and incubated for 3 days at the indicated temperatures. Incubation at 14 °C was for 10 days. *C*, WT (MSUC-3D), *ypt6-2* (ZLY-2), and *ypt6*Δ (ZLY4) strains were grown at 25 °C to saturation. 3.0 μl of 10-fold diluted cultures, starting with 8×10^6 cells/ml, were spotted onto designated plates and incubated at the indicated temperatures for 2 days. *CFW*, calcofluor white (Fluorescent Brightener 28; Sigma)

Therefore, previous studies (7, 8, 11, 12) on the functional role of Ypt6p were performed with *ypt6* deletion or truncation mutants which are, however, sensitive to growth at elevated temperature. Since mutants lacking a given protein are sometimes able to adapt to such a situation by activating a by-path for example, we sought to investigate Ypt6p function in conditional mutants. By analogy with other heat-sensitive Ypt proteins, three single amino acid substitutions were introduced into the conserved (NKXD) sequence, known to be involved in nucleotide binding, and into the helical region following this sequence (Fig. 1*A*). Each of the three mutant alleles, *ypt6-1* (expressing Ypt6(K125N)p), *ypt6-2* (expressing Ypt6(G139D)p), and *ypt6-3* (expressing Ypt6(A143D)p), conferred heat sensitivity to a varying extent on haploid cells grown in rich media (Fig. 1*B*). *ypt6-2* cells exhibited the most severe growth defect. Like *ypt6*Δ cells of the same genetic background, this mutant grew slowly at 35 °C and failed to proliferate at 37 °C. The *ypt6-1* mutant grew well at 37 °C but extremely slowly at 39 °C, whereas growth of *ypt6-3* cells slowed down at 37 °C and completely failed at 39 °C. Compared with wild type, all *ypt6* mutants exhibited somewhat reduced growth at 14 °C.

The growth defects of *ypt6* mutants at high temperature were partially rescued by the addition of 1 M sorbitol, a phenotype described for mutants with a defective cell wall (29). Therefore, we tested whether *ypt6* mutants are sensitive to SDS and calcofluor white (CFW), agents affecting cell wall integrity and being more toxic to mutants with a defective cell wall. Compared with the wild type strain, *ypt6-2* and *ypt6* null mutants were more sensitive to 0.005% SDS and 0.005% CFW (Fig. 1*C*), indicating a cell wall defect in these mutants.

Protein Trafficking Defects in ypt6 Mutants—We selected vacuolar carboxypeptidase Y (CPY), alkaline phosphatase (ALP), and the secreted invertase as markers to test whether the intracellular vesicle transport was affected in the *ypt6* mutants. These three proteins are *N*-linked glycoproteins that undergo core glycosylation in the ER and outer chain elongation in the Golgi before being transported to their final destination via different routes. CPY is transported via endosomes to the lumen of the vacuole, where it is processed to the mature form by proteolysis (30). ALP is transported directly to the membrane of the vacuole without passing through endosomes (31) and is also cleaved by proteolysis in the vacuole. Invertase is rapidly transported to the periplasmic space (32). By monitoring the molecular size and/or localization, it can be determined which step of transport is affected in the mutants. At steady state, accumulation of core-glycosylated CPY (p1-form) was detected in *ypt6-1, ypt6-2,* and *ypt6-3* when shifted to the nonpermissive temperature (37 or 39 °C) for 1 and 2 h (Fig. 2*A*). Further kinetic analysis of CPY by pulse-chase experiments showed that at permissive temperature (25 or 30 °C), *ypt6* mutants exhibited somewhat delayed maturation of the enzyme and a partial mis-sorting of the Golgi-glycosylated p2 form to the extracellular space. At nonpermissive temperature, *ypt6* mutants exhibited significantly reduced CPY transport kinetics. However, defects in the Golgi-specific glycosylation were demonstrated by the presence of a smear between p2CPY and p1CPY (compare wild type and mutants in Fig. 2, *B* and *C*). This is best seen in the experiment shown in Fig. 2*C* in which cells initially grown at 25 °C were taken up in SMM containing 1 M sorbitol for cell stabilization, preincubated at either 25 or 37 °C for 10 to 60 min, and then radioactively labeled for 10 min at the respective temperature. Although the extent of CPY labeling decreased with the length of time the cells were incubated in the hypertonic medium, mis-sorting of a significant fraction of the Golgi-glycosylated vacuolar enzyme was evident already 10 min after shift of *ypt6-2* cells to the nonpermissive temperature, and the p2 form of CPY decreased in size at later time points. At 60 min of preincubation at 37 °C, p2-CPY of the *ypt6-2* mutant cells, in contrast to wild type cells, was detectable only as a smear above the sharp band of the ER core-glycosylated enzyme, clearly demonstrating a severe glycosylation defect in the Golgi. The defects observed in *ypt6-2* mutants were more severe than those in *ypt6-1* and *ypt6-3* cells, consistent with the growth phenotype. As shown in Fig. 3*A*, pro-ALP was also accumulated in *ypt6* mutants at steady state upon shift to nonpermissive temperature. Further analysis by pulse-chase experiments indicated that at 25 °C, maturation of ALP was normal in *ypt6-2* mutant cells. However, at 37 °C, pro-ALP was accumulated and, in gels, migrated progressively slower at chase times from 0 to 30 min (Fig. 3*B*), suggesting ongoing glycosylation in the Golgi.

Invertase was analyzed both in the intracellular and extracellular fraction by activity staining in non-denaturing polyacrylamide gels. At permissive temperature, the secretion of highly glycosylated invertase was normal in *ypt6* mutants as compared with wild type cells. At nonpermissive temperature, *ypt6-1* and *ypt6-3* mutants showed slight defects in the secretion and glycosylation of the enzyme. Importantly, at 37 °C invertase in *ypt6-2* mutant cells was clearly underglycosylated, and somewhat less than half of the enzyme was accumulated inside the cell. As controls for ER-to-Golgi transport mutants, processing and secretion of invertase was investigated in *sec18-1* and *ypt1*^{A136D} strains at nonpermissive conditions. In these mutants, the enzyme was nearly completely trapped inside the cells in ER-glycosylated forms (Fig. 4*A*). To analyze further whether Ypt6p is involved in secretion, we assayed for the export of proteins into the growth medium (24, 26). Wild type and mutant cells were preincubated at 37 °C for 30 min

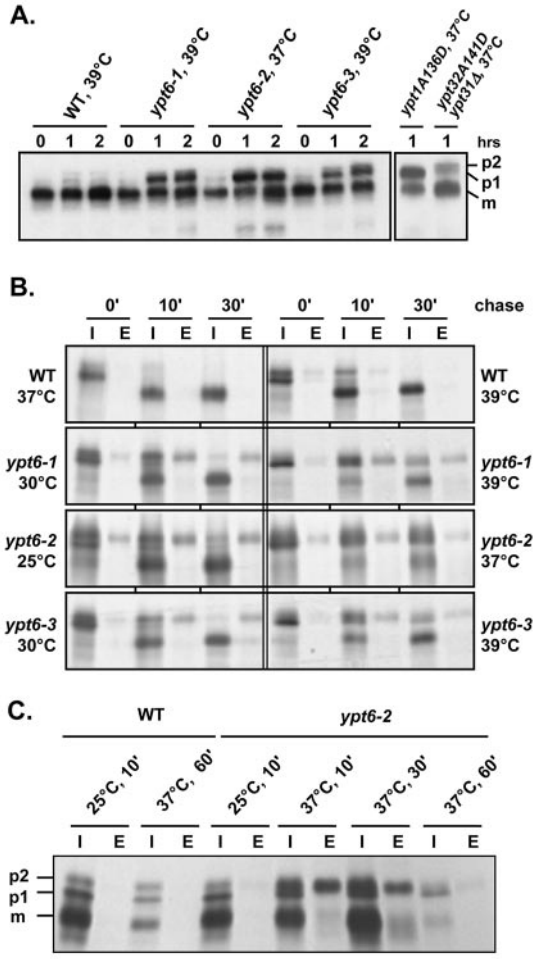

FIG. 2. **CPY transport analysis in *ypt6* mutants.** *A*, Western blot analysis of CPY with total protein extracts. WT (MSUC-3D), *ypt6-1* (ZLY1), *ypt6-2* (ZLY2), *ypt6-3* (ZLY3), *ypt1*^{A136D} (YXY136), and *ypt32*^{A141D}/*ypt31*Δ (YLX15) cells were grown at 25 °C to mid-log phase and shifted to 37 or 39 °C for 0, 1, or 2 h before lysis. After SDS-PAGE, transfer to nitrocellulose filters and treatment with anti-CPY antibody, CPY was visualized by fluorography. *B*, pulse-chase analysis with WT (MSUC-3D) and *ypt6* mutants (ZLY1, ZLY2, and ZLY3). Cells were either incubated at permissive temperature or shifted to nonpermissive temperature for 30 min in SD medium containing required amino acids and 1 mg/ml of ovalbumin, labeled for 7 min with Tran^{35}S-label, and then chased with cold methionine and cysteine for the indicated times. The cells were then spheroplasted, and intracellular (*I*) and extracellular (*E*) fractions were collected. CPY was immunoprecipitated from both fractions, resolved by SDS-PAGE, and visualized by autoradiography. Note that mis-sorting of CPY occurred already at permissive temperatures. *C*, WT and *ypt6-2* mutant cells were preincubated in SMM containing 1 M sorbitol and 1 mg/ml ovalbumin at the indicated times and temperatures, labeled with Tran^{35}S-label for 10 min, and chased for 30 min. Newly synthesized CPY was identified as described in *B*.

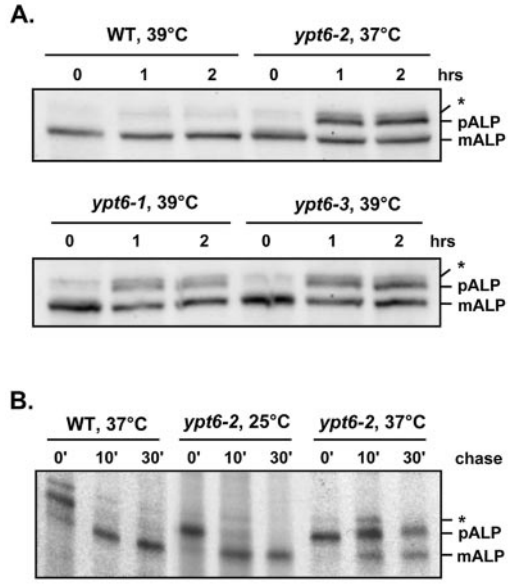

FIG. 3. **ALP maturation in *ypt6* mutants.** *A*, Western blot analysis of ALP with total cellular protein. The same extracts used in the experiment of Fig. 2*A* were analyzed with anti-ALP antibody. *B*, pulse-chase analysis with WT (MSUC-3D) and *ypt6-2* (ZLY2) mutants. Cells were grown and subjected to pulse-chase analysis as described in the legend to Fig. 2*B*. ALP was immunoprecipitated from cell lysates, resolved by SDS-PAGE, and visualized by autoradiography. * denotes an unrelated protein band that does not change electrophoretic behavior after PNGase F treatment.

and then subjected to pulse-chase at 37 °C. Cells were removed by centrifugation, and the proteins in the medium were precipitated with trichloroacetic acid, resolved by SDS-PAGE, and identified by autoradiography. As shown in Fig. 4*B*, no protein band was detected in the medium of *sec18-1* cells, and only very faint bands were seen in the medium of *ypt1*^{A136D} cells, indicating the known secretion block in these two mutants. However, the same set of secreted proteins, including the most prominent band at 130–150 kDa that represents HSP150 (24, 26), was visible in the medium of wild type, *ypt6-2,* and *ret2-1* cells, the latter being defective in retrograde transport from the Golgi to the ER (33). Comparing the band intensities, it appears that secretion in *ypt6-2* mutants was somewhat reduced.

We next examined the recycling of the v-SNARE Sec22p in *ypt6-2* mutant cells. Sec22p is known to cycle between the Golgi and the ER as well as between Golgi compartments. In wild type cells, only a small fraction of the v-SNARE reaches the late Golgi, but in mutants defective in retrograde transport of ER resident proteins, Sec22p is easily mis-sorted to this compartment (34, 35) in which the Kex2 protease resides. For this study, we took advantage of an Sec22-α factor fusion protein with a Kex2p cleavage site in its linker region and a c-Myc epitope tag adjacent to Sec22p. Cleavage of the fusion protein signals arrival in the late Golgi (34). As shown in Fig. 4*C*, the fraction of the fusion protein cleaved was significantly higher in *ypt6-2* mutant cells compared with wild type cells independent of the temperature at which the experiment was conducted. This clearly indicates a recycling defect in Ypt6p-defective cells that could involve retrograde Golgi and/or Golgi-to-ER trafficking.

Glycosylation Defects of Golgi-localized Glycosyltransferases in ypt6-2 Mutants—The glycosylation defects of CPY and invertase in *ypt6* mutants prompted us to examine whether the defects resulted from instability of glycosyltransferases. In yeast cells, outer chain elongation of glycoproteins is catalyzed by glycosyltransferases in the Golgi. Among them, Anp1p, Mnn9p, and Van1p have been reported to recycle between the ER and the Golgi and are subject to mislocalization and to degradation in the vacuole when retrograde transport to the ER is blocked (36). We integrated c-Myc epitope-tagged versions of *ANP1, MNN9,* and *VAN1* into the genome of wild type and *ypt6-2* strains and followed the fate of the tagged proteins by immunoblot analysis. As shown in Fig. 5*A*, a shift of cells to 37 °C for 2 h did not result in a significant reduction of Anp1p-myc, Mnn9p-myc, and Van1p-myc in *ypt6-2* compared with wild type cells. Also no redistribution of Mnn9p-myc and Anp1p was detected in *ypt6-2* mutant cells in sucrose gradient analysis (Fig. 6*D*), suggesting other reason(s) for the glycosylation defects observed. Likewise, there was no decrease of the Golgi protein Emp47p following shift of *ypt6-2* cells to nonpermissive temperature (Fig. 5*A*).

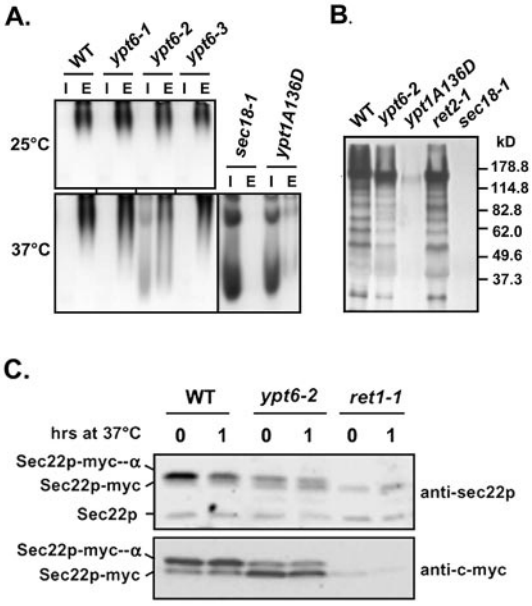

FIG. 4. **Secretion and Sec22p recycling analysis of *ypt6* mutants.** *A*, WT (MSUC-3D), *ypt6-1* (ZLY1), *ypt6-2* (ZLY2), *ypt6-3* (ZLY3), *sec18-1* (YTX50), and *ypt1*^{A136D} (YXY136) strains were grown at 25 °C to mid-log phase; and cells were washed and resuspended in 0.1% glucose-containing medium to induce secreted invertase at 25 or 37 °C for 1 h. Intracellular (*I*) and extracellular (*E*) fractions were separated, and invertase was analyzed by activity staining in non-denaturing acrylamide gels. *B*, WT (MSUC-3D), *ypt6-2* (ZLY2), *ypt1*^{A136D} (YXY136), *ret2-1* (PC130), and *sec18-1* (YTX50) strains were preincubated for 30 min at 37 °C, labeled for 10 min with Tran^{35}S-label, and then chased for 30 min. Proteins secreted into the medium were precipitated with trichloroacetic acid and analyzed by SDS-PAGE and autoradiography. *C*, recycling defect of Sec22p. WT (MSUC-3D), *ypt6-2* (ZLY2-K), and *ret1-1* (PC70) cells harboring the plasmid pWB-Acycα encoding Sec22p-myc-α factor (α) fusion protein were grown overnight at 25 °C to mid-log phase in SC-Ura medium, and then half of the cultures was shifted to 37 °C for 1 h. Total proteins were extracted from the cells before and after 1 h of treatment at 37 °C and analyzed by immunoblot using anti-Sec22p antibody or anti-c-Myc antibody. Sec22p-myc, the Kex2 protease cleaved products from Sec22p-myc-α fusion protein; Sec22p, wild type v-SNARE. Note that in the *ret1-1* mutant the fusion protein is almost completely cleaved.

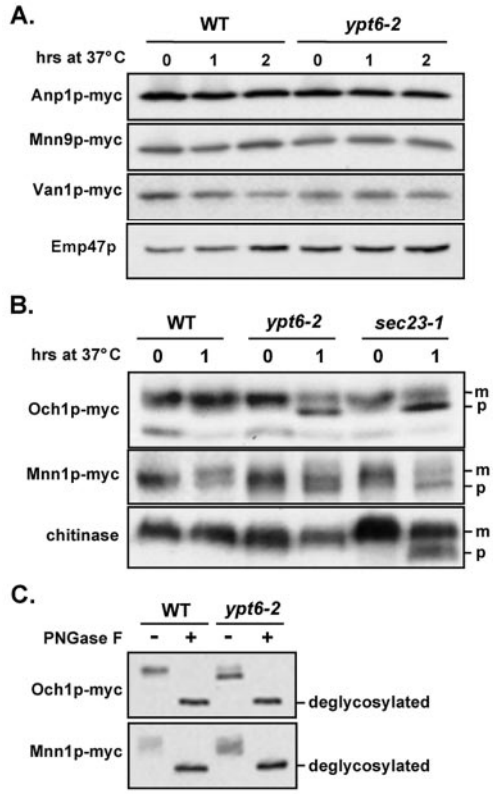

FIG. 5. **Western blot analysis of glycosyltransferases, Emp47p, and chitinase in *ypt6-2*.** *A*, stability of Myc-tagged Anp1p, Mnn9p, and Van1p. WT and *ypt6-2* strains expressing c-Myc-tagged Anp1p (ZLY354, ZLY359), Mnn9p (ZLY353, ZLY358), and Van1p (ZLY355, ZLY360) were grown at 25 °C to mid-log phase and shifted to 37 °C for 0, 1, or 2 h before lysis. Total proteins were analyzed by immunoblot using anti-c-Myc or anti-Emp47p antibodies. *B*, samples were prepared from WT, *ypt6-2,* and *sec23-1* strains expressing c-Myc-tagged Och1p (ZLY351, ZLY356, and ZLY184) and Mnn1p (ZLY352, ZLY357, and ZLY185) before or after shift to 37 °C for 1 h. Total proteins were subjected to immunoblot analysis using anti-c-Myc and anti-chitinase antibodies. *p*, core-glycosylated form; *m*, mature form. *C*, endoglycosidase treatment. WT and *ypt6-2* cells expressing c-Myc-tagged Och1p (ZLY351, ZLY356) or Mnn1p (ZLY352, ZLY357) were shifted to 37 °C for 1 h, and membrane proteins were extracted, treated with PNGase F, and visualized on Western blots using anti-c-Myc antibody.

Two other important glycosyltransferases are Och1p and Mnn1p. Och1p is the first enzyme required for outer chain elongation of *N*-linked glycoproteins in the *cis*-Golgi (37). It does not recycle back to the ER (36) but was reported to recycle between the TGN and the *cis*-Golgi (38). Mnn1p is responsible for the termination of both *N*- and *O*-linked glycosylation in the Golgi. It resides in two discrete Golgi compartments and may cycle between the earlier compartments and the TGN (39). To investigate whether Ypt6p might be involved in the recycling of Och1p and Mnn1p, we followed their fate by a similar strategy as described above. Two bands of Och1p-myc were detected in wild type, *ypt6-2,* and *sec23-1* cells at 25 °C. The upper broad band could in fact contain three bands, because Och1p was detected previously in four forms of 58–66 kDa (37). When cells were shifted to 37 °C for 1 h, a band about 1–2 kDa smaller than the upper broad band was accumulated both in *ypt6-2* and in *sec23-1* cells (Fig. 5*B*). Because in *sec23-1* cells, the exit of proteins from the ER is blocked, the additional band accumulating in the mutant cells was likely to represent the core-glycosylated form of Och1p-myc. This was confirmed by PNGase digestion, which removes all *N*-linked sugar chains from the protein (Fig. 5*C*). The core-glycosylated form of Mnn1p-myc was also detected in *ypt6-2* and *sec23-1* mutant cells after a shift to 37 °C (Fig. 5, *B* and *C*).

We also examined the extensively *O*-glycosylated protein chitinase that is located in the cell wall. Although the results of this investigation were somewhat variable, chitinase in *ypt6-2* mutant cells had no significantly altered electrophoretic mobility compared with wild type cells. However, accumulation of the ER form was seen only in *sec23-1* but not in *ypt6-2* mutant cells (Fig. 5*B*), again arguing against an inhibition of ER-to-Golgi transport in the *ypt6-2* mutant. These results indicate that in *ypt6-2* mutant cells, *N*-glycosylation in the Golgi is severely impaired, but *O*-glycosylation apparently is not.

Subcellular Localization of Core-glycosylated Forms of N-Linked Glycoproteins in ypt6-2 Mutants—We have shown that at steady state, the core-glycosylated forms of CPY, ALP, Och1p-myc, and Mnn1p-myc are accumulated in *ypt6* mutants at nonpermissive temperature. This accumulation may be the result of either a block in ER-to-Golgi transport as proposed previously (11) or may be caused by the lack of outer chain elongation of these glycoproteins. To distinguish between these possibilities, we performed a subcellular fractionation analysis, and we examined the localization of the underglycosylated and/or core-glycosylated proteins. Cell lysates were prepared from wild type, *ypt6-2,* and *sec23-1* strains carrying a Myc-tagged version of *OCH1*. After preincubation at 37 °C for 1 h, cells were collected, and lysates were prepared and subjected to sucrose gradient centrifugation. Following gel electrophoretic

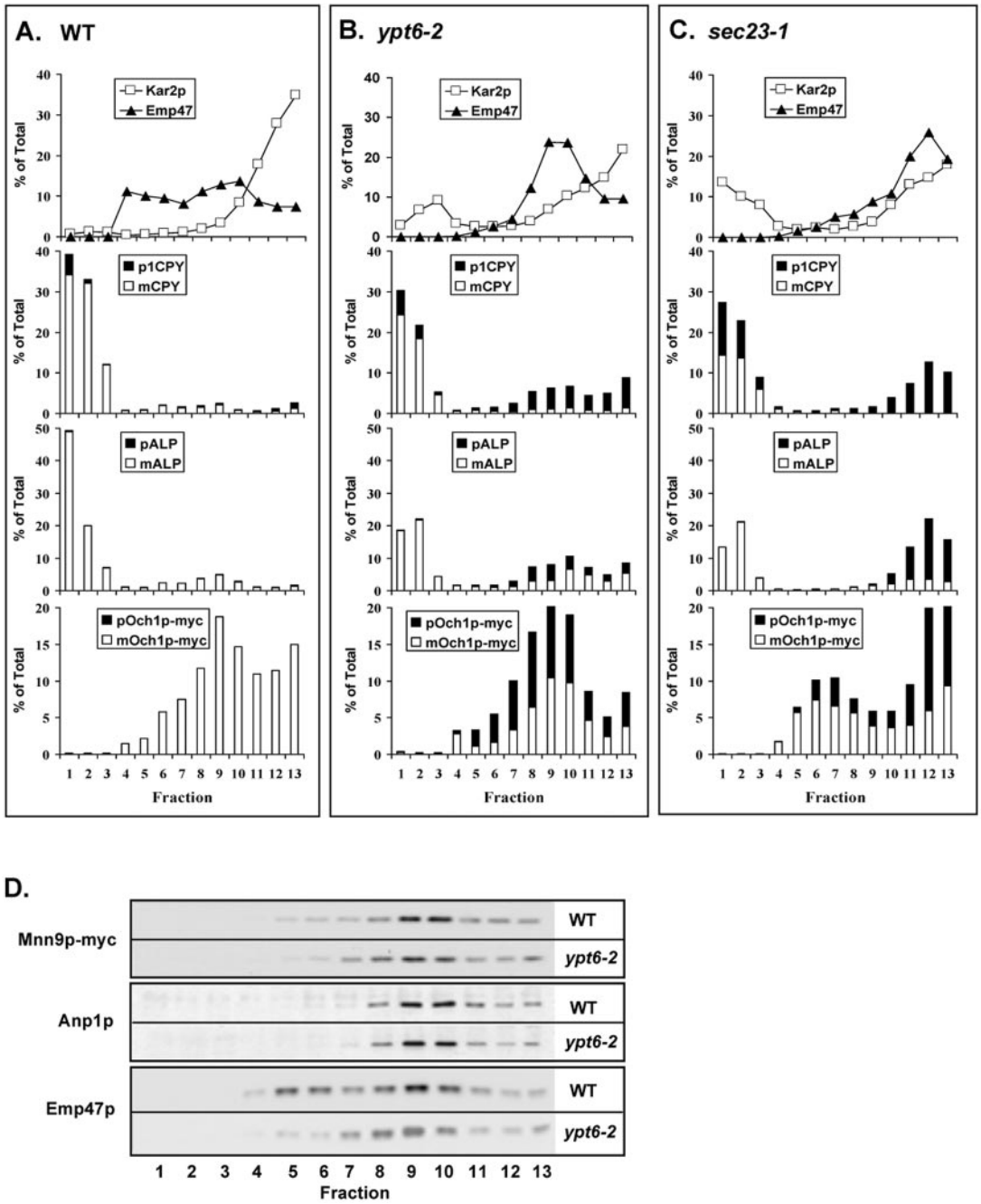

FIG. 6. **Distribution of proteins in sucrose gradients of *ypt6-2* lysates.** WT (*A*), *ypt6-2* (*B*), and *sec23-1* (*C*) strains expressing Myc-tagged Och1p (ZLY351, ZLY356, and ZLY184) were grown at 25 °C to mid-log phase and shifted to 37 °C for 1 h. Spheroplasts were generated and lysed gently. Lysates were fractionated by sucrose gradient (18–60%) centrifugation and assayed for the distribution of Och1p-myc, Emp47p, Kar2p, CPY, and ALP by immunoblot analysis using specific antibodies. Relative levels of proteins on immunoblots were quantified using a Lumi-Imager. *D*, WT and *ypt6-2* strains expressing Mnn9p-myc (ZLY353 and ZLY358) were used to make lysates and subjected to fractionation and immunoblot analysis as described above.

separation of proteins in different gradient fractions, immunoblot analyses were performed with specific antibodies against the Golgi membrane protein Emp47p, the soluble ER protein Kar2p, the vacuolar hydrolases CPY and ALP, and against the c-Myc epitope for the identification of Och1p-myc. Band intensities of immunoblots were quantified using a Lumi-Imager. As shown in Fig. 6*A*, in wild type cells, Kar2p was enriched in the three bottom fractions of highest sucrose density which contain ER and plasma membranes. The mature forms of CPY and ALP were in the three upper fractions of the gradient containing vacuoles and soluble proteins. Only very small fractions of core-glycosylated proforms were found. Emp47p that recycles between the Golgi and the ER (28) was distributed in two peaks between fractions 4 and 13 with the main peak in fractions 8–10 in most of the experiments. The peak of Och1p-myc was detected primarily in the latter fraction. In *sec23-1* cells with an inhibition of ER export, core-glycosylated proteins were mostly trapped in the ER as expected. This also applied to the proforms of CPY, ALP, and Och1p-myc that were particularly enriched in the three bottom fractions of the gradient (Fig. 6*C*). In addition, the peak of Emp47p was shifted to the ER membrane-containing region of the gradient. However, in *ypt6-2* mutant cells, most of the core- and underglycosylated forms of CPY, ALP, and Och1p-myc were distributed between fractions

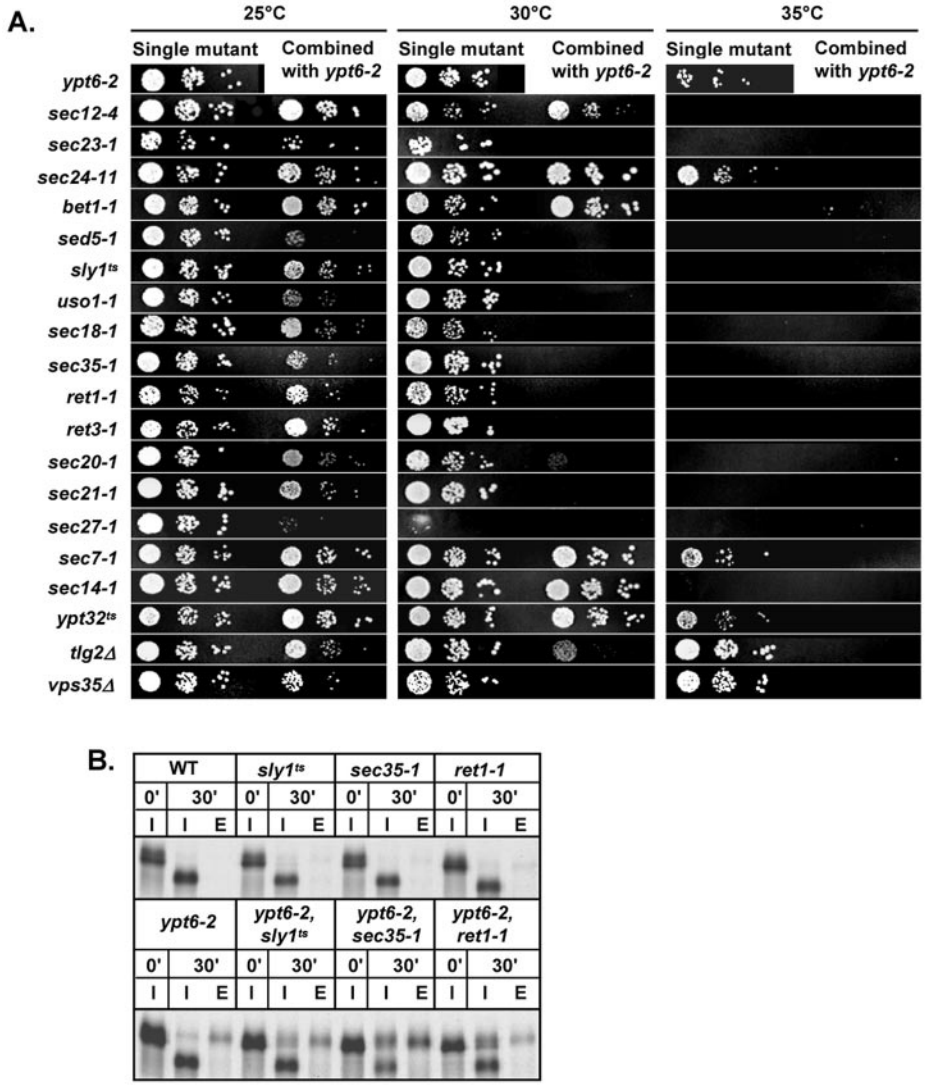

FIG. 7. **Genetic interactions between *ypt6-2* and other mutations.** *A*, *ypt6-2* (ZLY2) was combined with selected trafficking mutants by crossing ZLY2 with the respective strains (see Table I). Cells were grown at 25, 30, and 35 °C by spotting 10-fold diluted cultures onto YPD plates. *ypt32^{ts}* represents *ypt32^{A141D}*/*ypt31*Δ (YLX15). *B*, pulse-chase analysis of CPY. WT (MSUC-3D) and mutants (as indicated) were grown at 25 °C to mid-log phase, preincubated at 30 °C for 30 min, and then subjected to pulse-chase analysis at 30 °C as described in the legend to Fig. 2*B*.

6 and 13, with a peak around fractions 8–10, like the Golgi marker Emp47p (Fig. 6, *B* and *D*) and the Golgi-localized glycosyltransferases Mnn9p-myc and Anp1p (Fig. 6*D*). These results clearly indicate that most of the core-glycosylated proteins reached the Golgi cisternae in *ypt6-2* cells at nonpermissive temperature, arguing against a severe ER-to-Golgi trafficking defect.

We repeatedly observed that in the gradients used, Emp47p from cells grown at 37 °C for 1 h appeared in two peaks in contrast to *ypt6-2* cells where Emp47p was mostly confined to one peak coinciding with the Golgi glycosyltransferases (Fig. 6, *A*, *B* and *D*). As in the *ypt6-2* cells there is no indication for mis-sorting of Emp47p to the vacuole that would have been resulted in a decrease of the intracellular level of the protein (28), and this finding is probably due to a disturbance of Golgi homeostasis in cells defective in Ypt6p function.

Genetic Interactions of ypt6-2 and Mutants Defective in Transport between ER and Golgi or Endosomes and the TGN—Previous studies (7, 9, 12) had shown that overexpression of either Sys proteins, Ypt1p, Gos1p, or Ykt6p suppressed temperature-sensitive growth defects of *ypt6* null mutants. In the present study we could show that high intracellular levels of Sys1p and of Ypt1p efficiently rescued also the *ypt6-2* mutant from growth inhibition at 37 °C (data not shown). We additionally searched for synthetic growth defects between *ypt6-2* and other mutants defective in either ER-to-Golgi transport (*sec12-4, sec23-1, sec24-11, ypt1^{A136D}, yip1-2, sly1^{ts}, sed5-1, bet1-1, uso1-1, sec18-1,* and *sec35-1*), the Golgi-to-ER recycling (*ret1-1, ret2-1, ret3-1, sec20-1, sec21-1,* and *sec27-1*), intra- and post-Golgi transport (*sec7-1, ypt32^{A141D}*/*ypt31*Δ, and *sec14-1*), or in recycling between endosomes and the TGN (*tlg2*Δ and *vps35*Δ). Growth was examined at various temperatures by comparing double mutants with their parent strains (Fig. 7*A*).

Synthetic lethality, the phenomenon describing the inviability of double mutants that are viable with only one of the mutations, was observed when *ypt6-2* was combined with either *ypt1 ^{A136D}*, *yip1-2*, or *ret2-1*. Synthetic lethality usually indicates that the gene products concerned act in the same functional pathway. Ypt1-GTPase and Yip1p, a primarily Golgi-localized membrane protein binding Ypt1p and Ypt31p (40), are involved in docking/fusion of ER-derived vesicles with an early Golgi compartment, whereas Ret2p, the δ-subunit of COPI, principally acts in ER retrieval (33). Therefore, the results of the synthetic lethality screen suggested that Ypt6p might function, directly or indirectly, in anterograde and retrograde transport between the ER and the Golgi. The same conclusion could be drawn from other synthetic negative interactions shown in Fig. 7*A*. In particular, severe growth inhibition resulted from combining *ypt6-2* with conditional alleles of either *SED5* or *USO1* that encode the Golgi syntaxin and a vesicle tethering factor, respectively, for ER-to-Golgi forward transport. Synthetic negative effects on cell growth was also

observed by a combination of *ypt6-2* with temperature-sensitive alleles of either *SEC27* or *SEC21*, the genes for the COPI components β' and γ, respectively. Some of the mutant combinations were also tested for the maturation and sorting of newly synthesized CPY. We chose to combine *ypt6-2* with either *sly1^{ts}*, *ret1-1,* or *sec35-1*, mutants whose primary defects at nonpermissive temperature are either in ER-to-Golgi transport (41), in retrograde transport between Golgi compartments and the ER (42), or in more than one transport step (43), respectively. As can be seen in Fig. 7*B*, maturation and sorting of CPY was completely unaffected in *sly1^{ts}*, *ret1-1,* and *sec35-1* mutants at a permissive temperature of 30 °C, but combining either of these mutant alleles with *ypt6-2* resulted in an aggravation of the Golgi trafficking defect and the mis-sorting of CPY seen in the *ypt6-2* mutant alone. The strongest synthetic defects were seen in the *ypt6-2/sec35-1* double mutant. In addition, high expression of *SEC35* from a multicopy vector was found to partially rescue *ypt6-2* mutant cells from growth inhibition at 35 °C (data not shown), supporting the view that Sec35p and Ypt6p might act in the same pathway(s).

Severe synthetic growth defects were also observed when the *ypt6-2* allele was combined with either the deletion of *VPS35* or of *TLG2* (Fig. 7*A*). Although both deletions by themselves, or *ypt6-2* alone, allowed cell growth at 25, 30, and 35 °C, the double mutants did not grow at 35 °C and were completely (*ypt6-2/vps35*Δ) or severely (*ypt6-2/tlg2*Δ) growth-inhibited at 30 °C. As the syntaxin Tlg2p and the Vps35 protein are components of the machinery of endosome-to-Golgi trafficking, these results are in line with the conclusions drawn from previous studies (7–10, 13) indicating that Ypt6p has a function also in recycling between endosomes and the TGN.

DISCUSSION

Previous studies on the role of Ypt6p in intracellular protein transport have led to two quite different models, one suggesting an involvement of this GTPase in recycling between endosome(s) and the *trans*-Golgi (7, 8), and the other postulating a regulatory role in anterograde transport between early Golgi compartments (11, 12). These models were originally built on the phenotypes that resulted from studies of *ypt6* null mutants or mutants expressing a C-terminally truncated Ypt6p. Although there is experimental support for the first of the two models (9, 10), it has been difficult to establish the primary role for Ypt6p because permanent loss of the GTPase may result in cells bypassing the requirement for Ypt6p or in masking certain defects. An instructive example for such a situation is the loss of clathrin heavy chain function in yeast which results in mis-sorting of vacuolar proteins immediately after clathrin inactivation, whereas in cells lacking functional clathrin heavy chain, vacuolar protein sorting is restored (44). With this in mind, temperature-sensitive *ypt6* mutants were created of which one, *ypt6-2*, was growth-inhibited already at 35 °C.

Our findings that at nonpermissive temperatures heat-sensitive *ypt6* mutants accumulate apparently core-glycosylated CPY, ALP, and Myc epitope-tagged Golgi mannosyltransferases Och1p and Mnn1p, and that synthetic lethality results from combining the *ypt6-2* mutant allele with either the *ypt1^{A136D}* or the *yip1-2* allele seemed to support a role of Ypt6p played in anterograde ER-to-Golgi transport. However, further analysis of transport kinetics of CPY and ALP by pulse-chase experiments revealed that the accumulated proforms of CPY and ALP resulted from underglycosylation rather than from a defect in ER-to-Golgi transport. This was further confirmed by subcellular fractionation analysis of *ypt6-2* mutants that showed Golgi localization of core-glycosylated vacuolar and Golgi-resident enzymes. By following the fate of newly synthesized secreted proteins at nonpermissive temperature, it became evident that a substantial fraction of them reached the extracellular space, indicating that they had passed the Golgi.

How might rapid loss of Ypt6p function cause Golgi glycosylation defects? One possibility could be that Ypt6p is required for proper functioning, stability, or localization of glycosyltransferases. However, in *ypt6-2* mutant cells shifted to nonpermissive temperatures for up to 2 h, we did not find a significant decrease in the steady-state level of the Golgi glycosyltransferases Anp1p, Mnn9p, or Van1p, but we observed underglycosylation of the Golgi mannosyltransferases Och1p and Mnn1p at steady state already 1 h after temperature shift. Although there is no evidence for the *N*-glycans being essential for the functioning of these glycosyltransferases, proper localization of the *cis*-Golgi mannosyltransferase Och1p has been shown previously to involve a retrograde transport pathway from late to early Golgi compartments (38), and Mnn1p, which is apparently localized to two distinct Golgi compartments, was also proposed to cycle between late and early Golgi compartments (39, 45). It therefore appears likely that a primary role of Ypt6p is in retrograde Golgi transport, including the recycling of Golgi glycosyltransferases which, when disturbed as in conditional *ypt6* mutants, would interfere with their proper localization and hence result in protein glycosylation defects and a slow down of anterograde transport. Importantly, glycosylation defects were not detected in *ypt6* deletion mutants at permissive temperature (9, 11), which would have been expected given the role proposed here for the GTPase. An explanation for this apparent discrepancy could be that altered distribution or functional impairment of glycosyltransferases in permanently Ypt6p-lacking cells is compensated for by an increase of ER-to-Golgi trafficking activity. Rescue of *ypt6* deletion mutants from growth inhibition at high temperature through intracellular levels of Ypt1p or the expression of *SLY1-20* (12), which we also observed with the temperature-sensitive *ypt6-2* in the present study, support this assumption. The apparent impairment of ER-to-Golgi traffic that we have observed in the conditional *ypt6* mutant at nonpermissive temperature, therefore, is likely to be a secondary effect.

In support of an involvement of Ypt6p in retrograde Golgi transport is our genetic data demonstrating synthetic lethality or severe synthetic negative growth defects after combining the *ypt6-2* mutant allele with either mutant alleles of various genes encoding subunits of the COPI complex or with *sec35-1*. Sec35p is part of a multicomponent protein complex (43, 46, 47), the primary function of which appears to be in tethering vesicles in retrograde Golgi transport. Components of this tethering complex have also been discussed to act in an endosome-to-Golgi protein retrieval (43, 48). Interestingly, our study revealed genetic interactions between the *ypt6-2* mutant allele and deletions of either *TLG2* or *VPS35*, nonessential genes whose protein products have been documented previously to fulfill functions in the recycling of proteins from endosomes to the Golgi (49–53).

Collectively, the biochemical and genetic data obtained with the temperature-sensitive *ypt6* mutants indicate that the GTPase Ypt6p exerts its presumably regulatory role in vesicular protein transport from endosome(s) to the Golgi as well as in retrograde trafficking between Golgi compartments. Although the involvement of Ypt6p in several transport steps from endosome(s) to early Golgi compartments had been postulated from studies undertaken previously (7–10), it is the generation and analysis of the first conditional *ypt6* mutants that allowed us to observe the rather fast kinetics of transport disturbances, defects in protein glycosylation by Golgi mannosyltransferases and in protein sorting in the late Golgi follow-

ing Ypt6p inactivation. Further detailed analyses of Ypt6p function have to await the generation of cell-free systems, allowing the differentiation between different transport steps, but this will be a difficult task given the complexity of protein recycling between compartments of the endocytic pathway and the Golgi complex (54). Interestingly, after several years of investigating Rab6, the mammalian counterpart of Ypt6p, it seems certain now that in mammalian cells, retrograde transport from endosomes to the *trans*-Golgi network and from late to early Golgi compartments (and possibly to the ER) is also controlled by this GTPase although in the form of two different isoforms (16–18). The Sec22p recycling defect that we have observed in the present study underlines the importance of Ypt6p in retrograde Golgi transport and, together with some of the genetic data obtained, leaves open the possibility that Ypt6p is effective also in retrograde transport from the Golgi to the endoplasmic reticulum.

Acknowledgments—We thank Hans Dieter Schmitt, Renwang Peng, and Xiaoping Yang for helpful discussions and for providing yeast strains and plasmids; Ludwig Lehle (University Regensburg) for anti-chitinase antibody; Sean Munro (MRC Cambridge) for anti-Anp1p antibody; Rita Schmitz-Salue for technical assistance; Hans-Peter Geithe for sequencing; and Ingrid Balshüsemann for secretarial help.

REFERENCES

1. Jahn, R., and Sudhof, T. C. (1999) *Annu. Rev. Biochem.* **68,** 863–911
2. Mellman, I., and Warren, G. (2000) *Cell* **100,** 99–112
3. Lazar, T., Gotte, M., and Gallwitz, D. (1997) *Trends Biochem. Sci.* **22,** 468–472
4. Pfeffer, S. R. (2001) *Trends Cell Biol.* **11,** 487–491
5. Segev, N. (2001) *Curr. Opin. Cell Biol.* **13,** 500–511
6. Zerial, M., and McBride, H. (2001) *Nat. Rev. Mol. Cell Biol.* **2,** 107–117
7. Tsukada, M., and Gallwitz, D. (1996) *J. Cell Sci.* **109,** 2471–2481
8. Tsukada, M., Will, E., and Gallwitz, D. (1999) *Mol. Biol. Cell* **10,** 63–75
9. Bensen, E. S., Yeung, B. G., and Payne, G. S. (2001) *Mol. Biol. Cell* **12,** 13–26
10. Siniossoglou, S., and Pelham, H. R. (2001) *EMBO J.* **20,** 5991–5998
11. Li, B., and Warner, J. R. (1996) *J. Biol. Chem.* **271,** 16813–16819
12. Li, B., and Warner, J. R. (1998) *Yeast* **14,** 915–922
13. Siniossoglou, S., Peak-Chew, S. Y., and Pelham, H. R. (2000) *EMBO J.* **19,** 4885–4894
14. Cao, X., Ballew, N., and Barlowe, C. (1998) *EMBO J.* **17,** 2156–2165
15. Jedd, G., Richardson, C., Litt, R., and Segev, N. (1995) *J. Cell Biol.* **131,** 583–590
16. Martinez, O., Schmidt, A., Salamero, J., Hoflack, B., Roa, M., and Goud, B. (1994) *J. Cell Biol.* **127,** 1575–1588
17. Mallard, F., Tang, B. L., Galli, T., Tenza, D., Saint-Pol, A., Yue, X., Antony, C., Hong, W., Goud, B., and Johannes, L. (2002) *J. Cell Biol.* **156,** 653–664
18. White, J., Johannes, L., Mallard, F., Girod, A., Grill, S., Reinsch, S., Keller, P., Tzschaschel, B., Echard, A., Goud, B., and Stelzer, E. H. (1999) *J. Cell Biol.* **147,** 743–760
19. Gietz, D., St Jean, A., Woods, R. A., and Schiestl, R. H. (1992) *Nucleic Acids Res.* **20,** 1425
20. Sherman, F., and Hicks, J. (1991) *Methods Enzymol.* **194,** 21–37
21. De Antoni, A., and Gallwitz, D. (2000) *Gene* (*Amst.*) **246,** 179–185
22. Sikorski, R. S., and Hieter, P. (1989) *Genetics* **122,** 19–27
23. Baudin, A., Ozier-Kalogeropoulos, O., Denouel, A., Lacroute, F., and Cullin, C. (1993) *Nucleic Acids Res.* **21,** 3329–3330
24. Gaynor, E. C., and Emr, S. D. (1997) *J. Cell Biol.* **136,** 789–802
25. Reid, G. A. (1983) *Methods Enzymol.* **97,** 324–329
26. Peyroche, A., and Jackson, C. L. (2001) *Methods Enzymol.* **329,** 290–300
27. Benli, M., Doring, F., Robinson, D. G., Yang, X., and Gallwitz, D. (1996) *EMBO J.* **15,** 6460–6475
28. Schröder, S., Schimmoller, F., Singer-Kruger, B., and Riezman, H. (1995) *J. Cell Biol.* **131,** 895–912
29. Cid, V. J., Duran, A., del Rey, F., Snyder, M. P., Nombela, C., and Sanchez, M. (1995) *Microbiol. Rev.* **59,** 345–386
30. Stevens, T., Esmon, B., and Schekman, R. (1982) *Cell* **30,** 439–448
31. Piper, R. C., Bryant, N. J., and Stevens, T. H. (1997) *J. Cell Biol.* **138,** 531–545
32. Esmon, B., Novick, P., and Schekman, R. (1981) *Cell* **25,** 451–460
33. Cosson, P., Demolliere, C., Hennecke, S., Duden, R., and Letourneur, F. (1996) *EMBO J.* **15,** 1792–1798
34. Ballensiefen, W., Ossipov, D., and Schmitt, H. D. (1998) *J. Cell Sci.* **111,** 1507–1520
35. Andag, U., Neumann, T., and Schmitt, H. D. (2001) *J. Biol. Chem.* **276,** 39150–39160
36. Todorow, Z., Spang, A., Carmack, E., Yates, J., and Schekman, R. (2000) *Proc. Natl. Acad. Sci. U. S. A.* **97,** 13643–13648
37. Nakayama, K., Nagasu, T., Shimma, Y., Kuromitsu, J., and Jigami, Y. (1992) *EMBO J.* **11,** 2511–2519
38. Harris, S. L., and Waters, M. G. (1996) *J. Cell Biol.* **132,** 985–998
39. Graham, T. R., Seeger, M., Payne, G. S., MacKay, V. L., and Emr, S. D. (1994) *J. Cell Biol.* **127,** 667–678
40. Yang, X., Matern, H. T., and Gallwitz, D. (1998) *EMBO J.* **17,** 4954–4963
41. Ossig, R., Dascher, C., Trepte, H. H., Schmitt, H. D., and Gallwitz, D. (1991) *Mol. Cell. Biol.* **11,** 2980–2993
42. Letourneur, F., Gaynor, E. C., Hennecke, S., Demolliere, C., Duden, R., Emr, S. D., Riezman, H., and Cosson, P. (1994) *Cell* **79,** 1199–1207
43. Whyte, J. R., and Munro, S. (2001) *Dev. Cell* **1,** 527–537
44. Seeger, M., and Payne, G. S. (1992) *EMBO J.* **11,** 2811–2818
45. Graham, T. R., and Krasnov, V. A. (1995) *Mol. Biol. Cell* **6,** 809–824
46. Ram, R. J., Li, B., and Kaiser, C. A. (2002) *Mol. Biol. Cell* **13,** 1484–1500
47. Suvorova, E. S., Duden, R., and Lupashin, V. V. (2002) *J. Cell Biol.* **157,** 631–643
48. Spelbrink, R. G., and Nothwehr, S. F. (1999) *Mol. Biol. Cell* **10,** 4263–4281
49. Abeliovich, H., Grote, E., Novick, P., and Ferro-Novick, S. (1998) *J. Biol. Chem.* **273,** 11719–11727
50. Seron, K., Tieaho, V., Prescianotto-Baschong, C., Aust, T., Blondel, M. O., Guillaud, P., Devilliers, G., Rossanese, O. W., Glick, B. S., Riezman, H., Keranen, S., and Haguenauer-Tsapis, R. (1998) *Mol. Biol. Cell* **9,** 2873–2889
51. Seaman, M. N., Marcusson, E. G., Cereghino, J. L., and Emr, S. D. (1997) *J. Cell Biol.* **137,** 79–92
52. Seaman, M. N., McCaffery, J. M., and Emr, S. D. (1998) *J. Cell Biol.* **142,** 665–681
53. Nothwehr, S. F., Bruinsma, P., and Strawn, L. A. (1999) *Mol. Biol. Cell* **10,** 875–890
54. Pelham, H. R., and Rothman, J. E. (2000) *Cell* **102,** 713–719
55. Peng, R., De Antoni, A., and Gallwitz, D. (2000) *J. Biol. Chem.* **275,** 11521–11528

MEMBRANE TRANSPORT STRUCTURE FUNCTION AND BIOGENESIS:

Biochemical and Genetic Evidence for the Involvement of Yeast Ypt6-GTPase in Protein Retrieval to Different Golgi Compartments

Zongli Luo and Dieter Gallwitz

J. Biol. Chem. 2003, 278:791-799.
doi: 10.1074/jbc.M209120200 originally published online October 24, 2002